

## CHAPTER 100

### VERTICAL WAVE BARRIERS: WAVE TRANSMISSION AND WAVE FORCES

David L. Kriebel<sup>1</sup>

#### ABSTRACT

Wave interaction with a vertical slotted wave barrier, also called a wave screen or slit-type breakwater, is considered. A theoretical analysis is presented based on application of the continuity, momentum, and energy equations to flow through the slots in the breakwater, accounting for head losses associated with flow constriction and re-expansion. As a result, relatively simple expressions are found for the wave transmission coefficient and for the wave forces on the wall. These are then verified by laboratory experiments with regular waves.

#### INTRODUCTION

Vertical-wall breakwaters are sometimes used to protect marinas and small boat harbors from both wind waves and boat wakes. These breakwaters encompass a variety of structures and have many names in the literature, including wave barriers, wave screens, and even wave "fences". In the Chesapeake Bay and other locations in the United States, these structures are most often built from marine lumber in the form of vertically-slotted walls extending to either full or mid-depth. Despite the growing use of such structures, however, relatively little comprehensive design information is available on either their wave transmission characteristics or on the wave forces that they would experience. As a result, these breakwaters have performed poorly in some instances, since even small gap spaces between the wall members allows a significant transmission of wave energy.

---

<sup>1</sup> Associate Professor of Ocean Engineering; Naval Architecture, Ocean, and Marine Engineering Dept.; United States Naval Academy; Annapolis, MD 21402

A definition sketch showing the plan-view of a slotted or slit-type vertical wave barrier with rectangular wall elements is shown in Figure 1. The primary variable defining the structure permeability is the porosity of the cross-section,  $P$ , defined as the ratio of the gap space,  $s$ , to the centerline-to-centerline spacing of the wall elements,  $s+b$ . Assuming that the wall is subjected to plane long-crested waves of height  $H_i$  with crests parallel to the wall, it is then of interest to describe the transmission coefficient,  $K_t = H_t/H_i$ , and the reflection coefficient,  $K_r = H_r/H_i$ , in terms of the porosity and in terms of the relative water depth and wave steepness. In addition, it is of interest to describe the wave force on one wall element,  $F$ , in either the positive or negative directions.

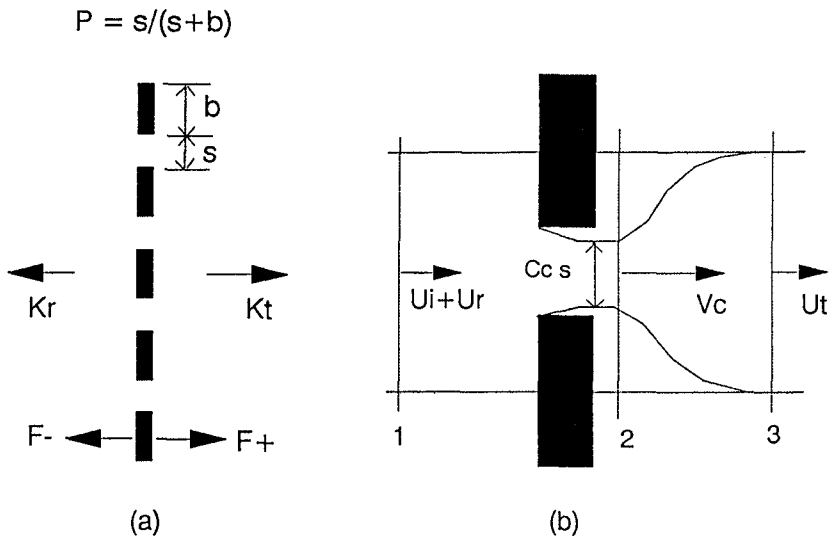


**Figure 1.** Definition sketch showing plan view of:  
(a) wall cross-section and (b) detail of flow through breakwater gap.

Vertical slotted or slit-type wave barriers have been actively studied for more than thirty years. Wiegel (1961), for example, estimated the transmission coefficient by assuming that the transmitted wave energy flux over width  $s+b$  was equal to that portion of the incident wave energy flux passing through the gap over width  $s$ . As a result, a simple expression for transmission was proposed as  $K_t = P^{1/2}$ . It is known, however, that this approach underestimates the transmission because it neglects the effects of wave reflection. In actuality, the pressure gradient across the wall is increased by the presence of the reflected wave and this drives more flow through the gap than is accounted for in Wiegel's method.

Recent analyses of these slit-type vertical wave barriers have been made using a variety of more complete analytical techniques. The most advanced solutions are based on potential flow methods and examples include the works of Kakuno (1983), Kojima et al. (1988), and Fugazza and Natale (1992). In these methods, the velocity potentials are found for the linear incident and reflected waves by applying both far field boundary conditions and matching conditions at the wall boundary. While solutions have been obtained for the wave transmission coefficient based on this approach, results have not been presented for the wave forces on the wall.

In contrast, simpler solutions based on fundamental hydraulics principles have also been proposed by Hayashi et al. (1966), Hayashi et al. (1968), Mei et al. (1974), Kondo (1979), and Urashima et al. (1986). These methods, also summarized by Mei (1983), have been developed for shallow water waves where wave pressures are hydrostatic and where flow velocities are uniform over depth. As a result, the equations for conservation of mass, momentum, and energy may be applied directly in two-dimensions in order to find the wave transmission coefficient. In most of these cases, solutions are also presented for the wave forces imparted on the wall by shallow water waves.

In the present paper, a hydraulic model similar to that of Hayashi et al. (1966) and Mei et al. (1974) is proposed for conditions of arbitrary water depth. It is assumed that both the wave transmission and wave forces are determined primarily by the strong horizontal fluid velocities that are driven through the breakwater gaps by the large pressure gradients that occur over the width of the wall. These maximum pressure gradients, and the associated maximum horizontal velocities, are largest during both the crest and trough phases of the wave. Because of this, it is assumed that the conservation equations can be applied first in horizontal layers and then depth-integrated to obtain the total wave transmission or the total wave force. Experimental verification of this simplified hydraulic theory is then presented based on recent laboratory experiments conducted at the U.S. Naval Academy.

## SIMPLIFIED HYDRAULIC THEORY

Consider the flow between two streamlines located along the centerline of adjacent wall elements and separated by width  $s+b$  as shown in Figure 1b. Conservation of mass requires the net discharge to be identical at each of the three sections shown in Figure 1b. As a result, the velocities at each of the three sections are related as:

$$u_i + u_r = C_c P V_c = u_t \quad (1)$$

where  $V_c$  is the velocity in the contraction and where  $C_c$  is the contraction coefficient, taken as  $C_c = 0.6 + 0.4P^3$  following Mei (1983). Based on linear wave theory, the velocities at the wave crest phase may then be given by

$$u_i = \sigma \frac{H_i}{2} Z_u \quad u_r = -\sigma \frac{H_r}{2} Z_u \quad u_t = \sigma \frac{H_t}{2} Z_u \quad (2)$$

where  $Z_u = \cosh(kh + kz) / \sinh(kh)$ ,  $k$  is the wave number,  $h$  is the water depth, and  $\sigma$  is the wave frequency. Because all velocities oscillate in time as  $\cos(\sigma t)$ , the wave heights are then related as

$$H_i - H_r = H_t \quad (3)$$

and the reflection and transmission coefficients are related as

$$K_r = 1 - K_t \quad (4)$$

Application of the momentum and energy equations then allows the pressure gradient across the wall to be determined. The momentum equation, applied between sections 2 and 3 in Figure 1b, is first used to find the pressure in the contraction in terms of the transmitted wave pressure and velocity. The energy equation, applied from section 1 to 2, is then used to relate the incident and reflected pressures to the pressure in the contraction. Combining these expressions, and using equation (1), finally yields the pressure drop across the wall as

$$p_i + p_r - p_t = \left(\frac{1}{C_c P} - 1\right)^2 \frac{1}{2} \rho u_t^2 \quad (5)$$

The right-hand-side of equation (5) represents the head loss through the gap as a quadratic function of the transmitted wave velocity. Following the method of equivalent linearization, e.g. Mei (1983), this may then be approximated as

$$p_i + p_r - p_t = K_{LOSS} \frac{4}{3\pi} \rho u_{tm} u_t \quad (6)$$

where  $u_{tm}$  is the magnitude of the transmitted wave velocity and where  $K_{LOSS}$  is the head loss coefficient. This is given as  $K_{LOSS} = ((1/C_c P) - 1)^2$  based on the flow constriction and expansion but will be modified later to account for other effects. As a result of the linearization, the velocities and pressures in equation (6) may be given by linear wave theory but the head loss on the right-hand-side will still retain a nonlinear effect of wave steepness.

SOLUTION FOR WAVE TRANSMISSION

The results presented above may now be extended into three dimensions to allow for variable pressures and velocities over the water depth, and to determine the overall transmission coefficient. Referring to Figure 2, it is first assumed that equation (6) models the pressure drop across the wall in any horizontal layer. It is further assumed that the dynamic pressures at any elevation are given by linear wave theory as

$$p_i = \rho g \frac{H_i}{2} Z_p \quad p_r = \rho g \frac{H_r}{2} Z_p \quad p_t = \rho g \frac{H_t}{2} Z_p \quad (7)$$

where  $Z_p = \cosh(kh + kz) / \cosh(kh)$ . Substitution of these expressions into equation (6), making use of equations (2) and (3), and integrating over depth then gives the following expression for wave transmission

$$\rho g H_i (1 - K_p) \int_{-h}^0 Z_p dz - K_{LOSS} \frac{1}{3\pi} \rho \sigma^2 H_i^2 K_t^2 \int_{-h}^0 Z_u^2 dz \quad (8)$$

The vertical integrations in this expression, from the seafloor  $z = -h$  to the still water level  $z = 0$ , are consistent with linear wave theory and account for the variable head losses over depth. As may be seen in Figure 2, the head losses are much larger near the surface than at the seafloor. It is also noted that by integrating to  $Z = 0$ , the head losses are assumed to be identical during both the crest and trough phases.

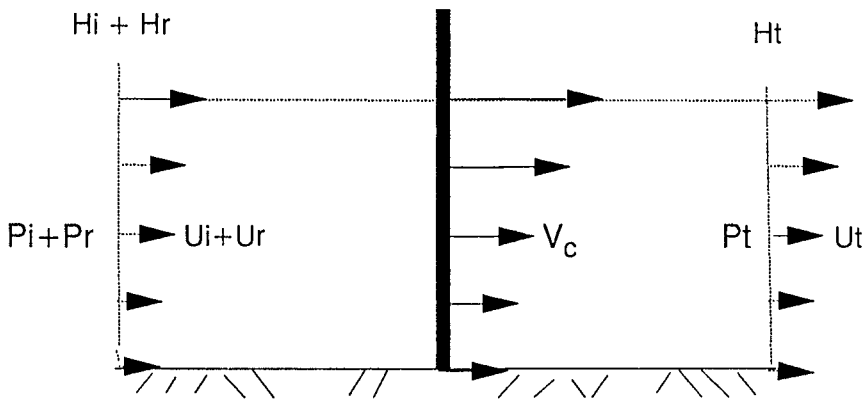


Figure 2. Illustration of vertical distribution of pressure and velocity.

Carrying out the operations in equation (8) ultimately yields a simple quadratic equation for the wave transmission coefficient as

$$T_t K_t^2 + K_t - 1 = 0 \quad (9)$$

where the variable  $T_t$  may be termed the *transmission function* and is equal to

$$T_t = K_{LOSS} \frac{1}{6} \frac{H_i}{L} \frac{\sinh 2kh + 2kh}{\sinh^2 kh} \quad (10)$$

The solution for wave transmission in arbitrary water depth is then found to have a form similar to that given by Mei (1983) in shallow water as

$$K_t = \frac{-1 + (1 + 4T_t)^{1/2}}{2T_t} \quad (11)$$

The solution for  $K_t$  in equations (10) and (11) contains the effects of both the relative water depth and the wave steepness, in addition to the breakwater porosity as reflected in the head loss coefficient. Figure 3 shows the variation in  $K_t$  as a function of porosity and relative depth for a fixed value of wave steepness. This shows that transmission is lower in shallow water than in deep water, because of the uniform velocities and therefore larger head losses over depth in shallow water. In addition, the transmission is essentially equal to that in deep water once  $h/L > 0.3$  or so. Figure 4 then shows the variation with wave steepness for deep water conditions. This illustrates that the head losses increase, and that the transmission decreases, for waves of higher steepness.

The functional dependencies on wave steepness and porosity may be displayed more clearly by considering deep water conditions, consistent with the experimental phase of this study, where  $T_t = K_{LOSS} H_i / 3L_o$  and where  $L_o$  is the deep water wavelength. As shown by Mei (1983, p. 263), the solution for wave transmission may be simplified based on series expansions of equation (11). For small amplitude waves or large gap spaces (small values of  $T_t$ ), it is found that

$$K_t = 1 - T_t = 1 - K_{LOSS} \frac{1}{3} \frac{H_i}{L_o} \quad (12)$$

On the other extreme, for large amplitude waves and narrow gap spaces (large values of  $T_t$ ), it may be shown that

$$K_t = \left( \frac{1}{T_t} \right)^{1/2} = \left( \frac{3}{K_{LOSS}} \frac{L_o}{H_i} \right)^{1/2} \quad (13)$$

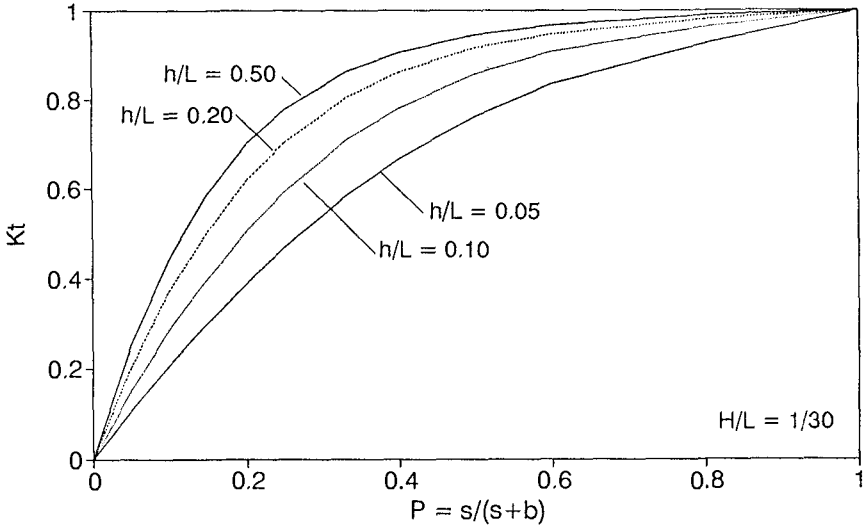


Figure 3. Example of wave transmission as a function of relative depth.

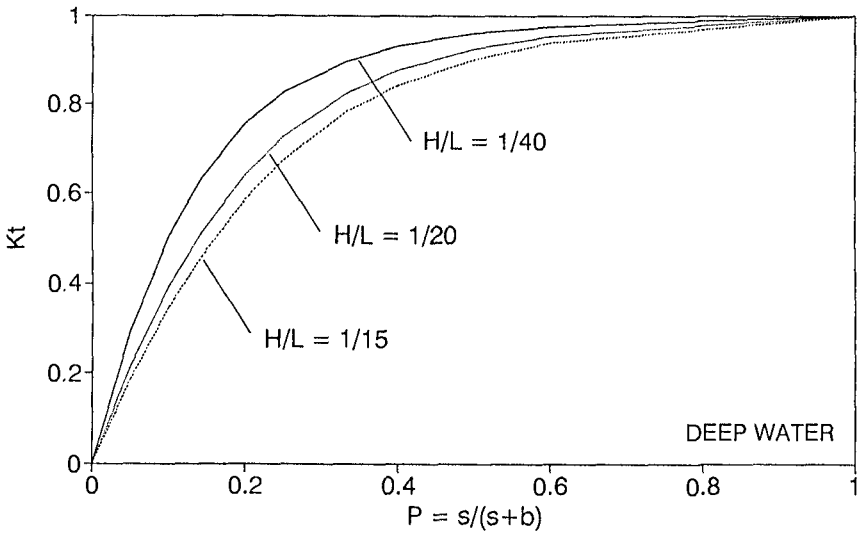


Figure 4. Example of wave transmission as a function of wave steepness.

## SOLUTION FOR WAVE FORCES

The wave force per unit length on one wall element,  $f$ , may be determined by applying the momentum equation from section 1 to 2 as shown in Figure 1b. Wave forces are then found from the differences in the specific forces on either side of the wall, assuming that the pressure in the contraction is impressed over the wake behind the wall. In water of arbitrary depth, this is applied to each fluid layer and the force per unit length is found to vary as

$$f = (p_i + p_r - p_t) (s+b) - \rho g H_i (1-K_r) Z_p (s+b) \quad (14)$$

Depth integration from the seafloor to the still water surface, consistent with linear wave theory, then gives the total force on one wall element,  $F$ , as

$$F = \rho g \frac{H_i}{k} \tanh(kh) (1-K_r) (s+b) \quad (15)$$

This expression is similar to the force exerted by linear standing waves on a solid wall of width  $b$ , denoted by  $F_o$  and given by

$$F_o = \rho g \frac{H_i}{k} \tanh(kh) b \quad (16)$$

As a result, the normalized force on one wall element of a slotted or slit-type vertical wave barrier may be expressed in the form

$$\frac{F}{F_o} = \frac{1 - K_r}{1 - P} \approx (1 - K_r)(1 + P) \quad (17)$$

where  $P$  is the wall porosity. According to equation (4), it is also found that the forces are directly proportional to the wave reflection coefficient. The maximum wave force reduces to the usual solution for linear standing waves when the wall porosity and the transmission coefficient approach zero. In general, however, the force on a permeable wall depends on the wall porosity, the relative depth, and the wave steepness, due to the dependence of the transmission coefficient on these parameters.

In the experimental phase of this study, wave forces were measured on walls with large gap spaces in some tests; and, in fact, some tests were performed on a single rectangular wall element placed in the center of the wave tank such that the porosity was essentially equal to unity. Under this extreme condition, the force on the wall element predicted by equation (17) is equal to zero. However, non-zero forces were measured and these measured forces were, as expected, well-represented by the Morison equation as the sum of drag and inertia forces.

Therefore, two empirical modifications of equation (17) were introduced. First, the inertia force on a rectangular wall element was included so that the total force on the wall was actually modelled as

$$\frac{F}{F_o} = (1-K_p)(1+P) \cos \sigma t - \pi C_m \frac{t}{L} K_t \sin \sigma t \quad (18)$$

where  $t$  is the wall thickness and  $C_m$  is the inertia coefficient, assumed to equal  $C_m = 1 + 0.325\pi b/t$  or 4.06 for rectangular members with a width-to-thickness ratio of 3 as used in this study. In addition, the head loss coefficient was modified as

$$K_{Loss} = \frac{3\pi}{16} C_D + \left( \frac{1}{C_c P} - 1 \right)^2 \quad (19)$$

where  $C_D$  is the viscous drag coefficient on a single rectangular element, assumed to equal two in this work. As the porosity approaches unity, the second term in equation (19) goes to zero and the first term then leads to the same drag force as would be found from the Morison equation, as may be shown based on the series expansion introduced in equation (12). On the other hand, as the porosity approaches zero, the second term governs and may be an order-of-magnitude larger than the first term.

## EXPERIMENTAL VERIFICATION

Verification of the theoretical results is based on physical model tests conducted at the United States Naval Academy Hydromechanics Laboratory in a wave tank 36.6 m long, 2.4 m wide, and 1.55 m deep, equipped with a flap-type wavemaker. A full-depth vertical wave barrier was constructed of wooden wall elements having a width,  $b = 7.62$  cm, and a thickness,  $t = 2.54$  cm. Five gap spacings were then tested, with  $s = 0.84, 1.27, 2.54, 3.81,$  and  $7.62$  cm. Single wall members were also tested. As a result, data is available for wall porosities  $P$  of 0.10, 0.14, 0.25, 0.33, 0.50, and 0.97.

Test were conducted using regular waves with four different wave frequencies, three of which produced deep water waves with  $h/L > 0.5$ . Deep water waves were considered here because many wave barriers are constructed in or adjacent to marinas or navigation channels where they are subjected to short-period wind waves or boat waves that are actually in deep water relative to their wavelength. At each frequency, up to three values of wave height were tested producing values of wave steepness of  $H/L = 1/40, 1/20,$  and  $1/15$ . Incident and transmitted waves were measured with fixed wave gages located near the wavemaker and 1 to 3 m behind the wall respectively. Wave forces were measured by attaching one of the vertical wall members, manufactured out of aluminum to provide additional stiffness, to a force gage.

## EXPERIMENTAL RESULTS

Examples of theoretical and experimental results for deep-water regular wave transmission are shown in Figure 5. In Figure 5a, transmission coefficients are shown for each of the four wave frequencies tested for a constant wave steepness of  $1/40$ . Figures 5b and 5c show similar results for a constant wave steepness of  $1/20$  and  $1/15$  respectively, although only three wave frequencies were actually tested at the higher steepness due to wavemaker limitations. As can be seen, the theory provides reasonable predictions of the transmission at all values of wall porosity and at all three values of wave steepness. In general, there was no discernable dependence in the data on wave frequency at a given value of porosity, consistent with the theoretical predictions. In addition, despite the linearizing assumptions made in the theory, predictions are quite good even for the higher wave steepness. One notable aspect of these results, however, is that for low steepness waves in deep water, wave transmission may be as high as 70 or 80 percent even for wall porosities of just 0.15 to 0.25.

Typical results for wave forces on the instrumented vertical wall element are shown in Figure 6. Figure 6a shows results for a wave steepness of  $1/40$  while Figure 6b shows results for a steepness of  $1/20$ . Measured forces reported here are actually the average of the positive and negative maximum forces, since the linear theory does not distinguish between force magnitudes at the crest or trough phase of the incident wave. The forces are then given in dimensionless form as the average measured force divided by the force predicted by linear standing wave theory. One result of this normalization, however, is that results differ for each wave frequency as porosity increases so that forces at different relative depths do not collapse to a single curve.

In Figure 6, it may be seen that the simplified hydraulic theory provides a reasonable estimate of measured forces for all values of porosity and for both values of wave steepness. Interesting features of the force predictions are that: (1) for very low values of porosity, predicted forces are mostly independent of relative depth and collapse to a single curve and that (2) once porosity exceeds about 0.5, dimensionless forces are nearly constant but differs for each relative depth. Reasons for this behavior may be seen in equation (18). At small values of porosity, the first term in equation (18) governs and, since the transmission coefficient is not a function of relative depth for these deep water conditions, the predicted dimensionless force is therefore the same for all frequencies tested. On the other hand, as the porosity becomes large, the second term in equation (18) governs and leads to a dependence of the dimensionless force on the wall thickness-to-wavelength ratio. It is noted that there is more scatter in the force data at the lower wave steepness since the measured forces for some of these conditions, particularly for  $h/L \approx 1.20$ , were very small and influenced by the sensitivity of the force gage

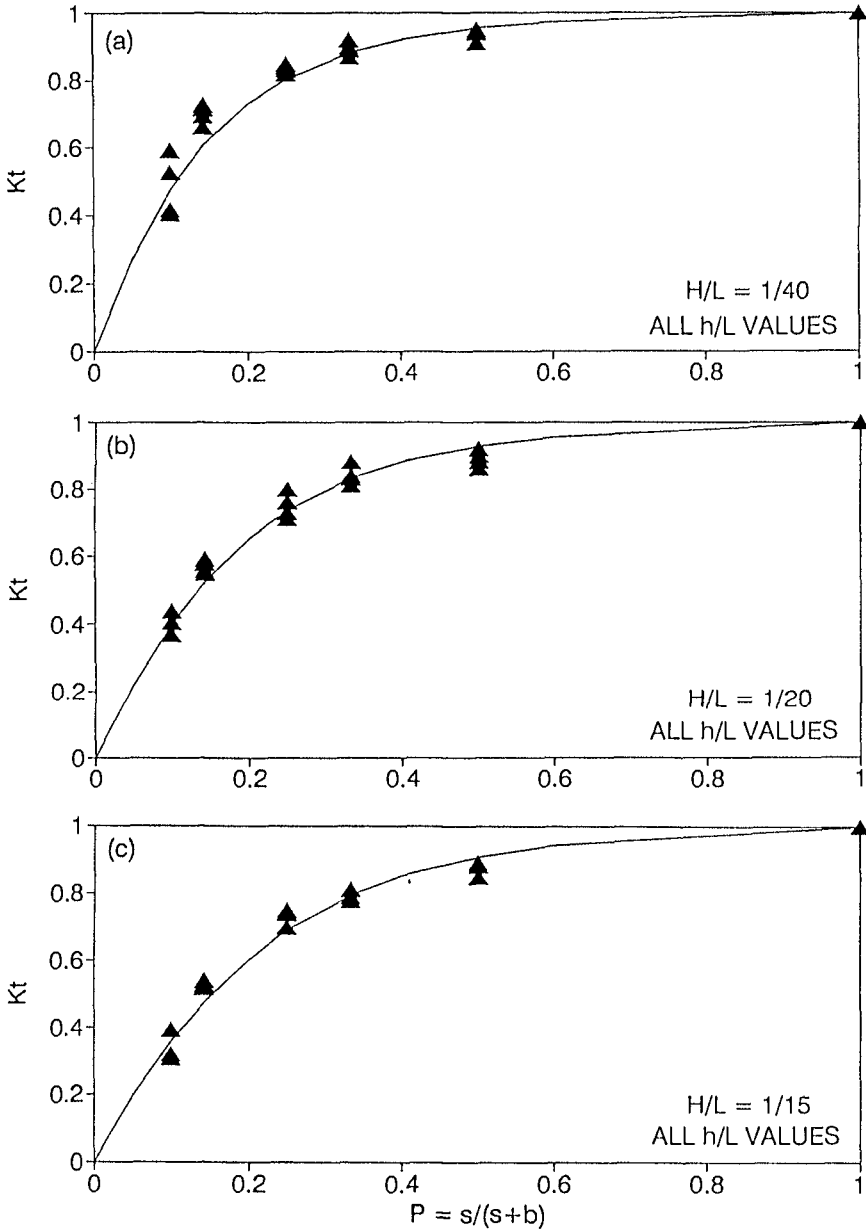
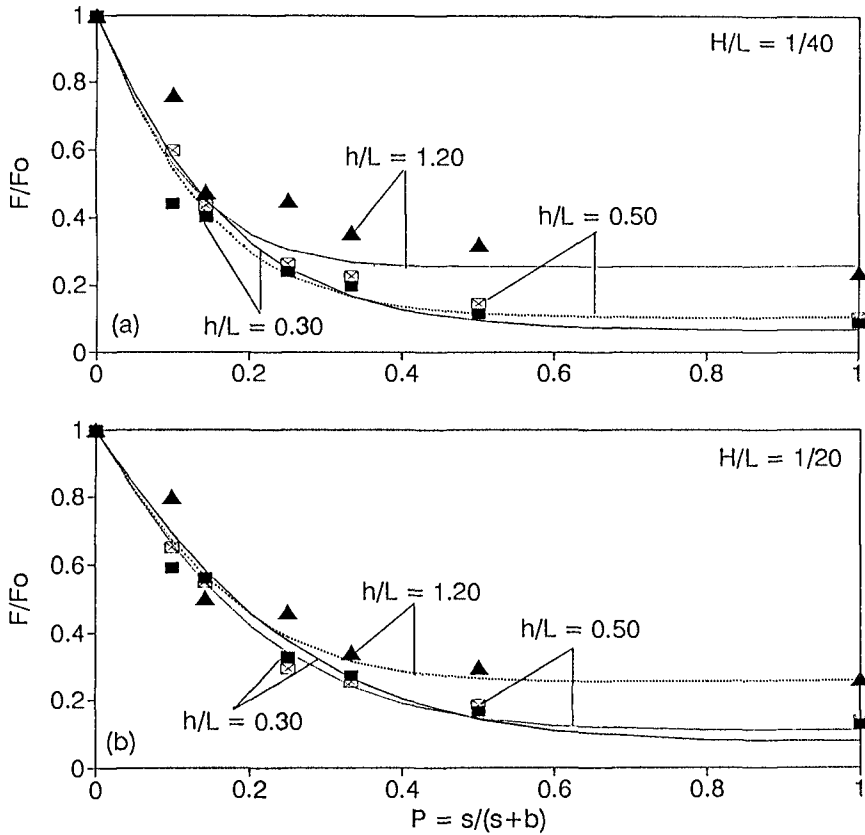


Figure 5. Comparison of measured and predicted deep water wave transmission. (a)  $H/L = 1/40$  and (b)  $H/L = 1/20$ , and (c)  $H/L = 1/15$ .



**Figure 6.** Comparison of measured and predicted deep water wave forces: (a)  $H/L = 1/40$  and (b)  $H/L = 1/20$ .

Some tests were also performed with random waves; however, space limitations prevent a complete discussion of these results. In general, it was found that the simplified hydraulic theory worked well for random wave transmission and wave forces when the significant wave height and peak wave period were used to characterize the random sea. As a single parameter, the significant wave height seemed to characterize the random sea better than the root-mean-square wave height. Apparently, the significant height gives a larger overall head loss that more closely approximates the actual head losses of the larger waves in a random sea.

## CONCLUSIONS

Methods presented in this paper allow a straightforward calculation of wave transmission and wave forces for a vertical slotted or slit-type wave barrier. As shown by both theory and experimental data, wave transmission decreases as the wave steepness increases and as the porosity decreases. However, wave forces increase under these same conditions. As a result, wave transmission can be decreased only at the expense of a large increase in the wave force on the wall. This trade-off between wave transmission and wave forces often leads to wall designs that are too porous and allow too much wave transmission in order to be economical to construct, particularly if the wall is to be attached to an existing pier as is often the case.

Under the assumption that both high wave transmission and high wave reflection are undesirable near marinas or entrance channels, the wall porosity associated with the maximum energy dissipation may be found. Based on an energy balance, the dissipated wave energy will equal

$$E_{DISS} = E_i - E_t - E_r = 2 E_i K_t (1 - K_t) \quad (20)$$

where equation (4) has been used to related  $K_r$  to  $K_t$ . As a result, it is found that the maximum wave energy dissipation occurs when  $K_t = 0.5$ . For values of wave steepness considered in this paper, and for deep water waves, this requires wall porosities in the range of 0.09 to 0.17 to maximize the energy dissipation. Based on constructed vertical wave barriers that the author has visited, porosities are generally larger than this by a factor of two or even three in some cases. Thus, the wave transmission coefficient is often more than 0.70 and is usually higher than intended or desired. Smaller gap spaces are therefore recommended when possible and where increased wave forces will not jeopardize the integrity of the supporting structure.

## ACKNOWLEDGEMENTS

This work was supported by the Ocean Technology Program of the National Science Foundation as part of a Presidential Young Investigator Award. The author would like to thank Louise Wallendorf of the Naval Academy Hydromechanics Laboratory and former students Laurie Wood, Troy McClelland, and Eric Thomas for carrying out the laboratory work. The author would also like to acknowledge several useful discussions with Robert G. Dean of the University of Florida who recently proposed a similar hydraulic model for wave transmission in an unpublished consulting report.

**REFERENCES**

- Fugazza, M., and Natale, L., 1992, "Hydraulic Performance of Perforated Breakwater," *Journal of Waterway, Port, Coastal, and Ocean Engr., ASCE*, Vol. 118, No. 1, pp. 1-14.
- Hayashi, T., Hattori, M., Kano, T., and Shirai, M., 1966, "Hydraulic Research on Closely Spaced Pile Breakwater," *Proc. 10th Intl. Conf. on Coastal Engr., ASCE*, pp. 873-884.
- Hayashi, T., Hattori, M., and Shirai, M., 1968, "Closely Spaced Pile Breakwater as a Protection Structure Against Beach Erosion," *Coastal Engineering in Japan*, Vol. 11, pp. 149-160.
- Kakuno, S., 1983, "Reflection and Transmission of Waves Through Vertical Slit-Type Structures," *Proc. Coastal Structures '83, ASCE*, pp. 939-953.
- Kojima, H., Ijina, T., and Yoshida, A., 1988, "A Numerical Method for Hydraulic Properties of a Slit-Type Breakwater Against Regular and Irregular Waves," *Proc. 6th Cong. Asian and Pacific Div. IAHR, Kyoto*, pp. 201-208.
- Kondo, H., 1979, "Analysis of Breakwaters Having Two Porous Walls," *Proc. Coastal Structures '79, ASCE*, pp. 962-977.
- Mei, C. C., 1983, "The Applied Dynamics of Ocean Surface Waves," *John Wiley & Sons, New York*.
- Mei, C., Liu, P., and Ippen, A., 1974, "Quadratic Loss and Scattering of Long Waves," *Journal of Waterways, Harbor, and Coastal Engr., ASCE*, Vol. 100, No. WW3, pp. 217-239.
- Urashima, S., Ishizuka, K., and Kondo, H., 1986, "Energy Dissipation and Wave Force at Slotted Wall," *Proc. 20th Intl. Conf. on Coastal Engr., ASCE*, pp. 2344-2352.
- Wiegel, R., 1961, "Closely Spaced Piles as a Breakwater," *Dock and Harbor Authority*, Vol. 42, No. 491, p. 150.